1.4.2 . Studies on the Arctic ozone depletion mechanisms using the chemical transport model

EF Fellow name: Alexander Lukyanov
Contact person: Hideaki Nakane
Deputy Director
Atmospheric Environmental Division
National Institute for Environmental Studies
Environment Agency
Onogawa 16-2, Tsukuba, Ibaraki 305, Japan
Tel. 81-298-50-2491, Fax. 81-298-58-2645
E-mail:nakane@nies.go.jp

Total Budget for FY 1996-FY 1998; 3, 705, 000 Yen (FY 1998;1, 837, 000Yen)

Abstract.
To simulate dynamical and chemical processes in the lower stratosphere the Lagrangian trajectory chemical model has been developed. This model is based on the chemical box model, developed in previous year, and trajectory model. Chemical species mixing ratio is integrated along large ensembles of isentropic or full three-dimensional calculated trajectories to produce the space distribution chemical picture in the region of interest. Reverse domain- filling technique provides the calculated values of the species on the uniform grid. The space resolution of the model depends on the number of trajectories only. In this study high latitude northern hemisphere in winter 1997 is considered.
Also model sensitivity studies have been conducted.

Keywords: Lagrangian Chemical Transport Model, Domain-filling trajectories, Polar Stratospheric Clouds, Heterogeneous chemistry

1. Introduction

It is now widely accepted that the polar stratospheric ozone depletion is primarily due to chlorine activation on the surface of Polar Stratospheric Clouds (PSCs). Under low temperature conditions chlorine reservoirs $ClONO_2$ and HCl are converted via heterogeneous reactions to temporal reservoirs Cl_2 and $ClNO_2$, which in presence of sunlight dissociate to active chlorine $Cl_x (= Cl + ClO + 2Cl_2O_2)$. However, this chlorine activation is in a strong competition with the process of $ClONO_2$ recovery.
Hydrolysis of N_2O_5 on sulfate aerosols and PSCs converts $NO_x (= NO + NO_2 + NO_3)$ to HNO_3, which dissociates very slowly in winter polar latitudes with temperature-dependent absorption cross section. This denoxification reduces the role of NO_x catalytic cycle of ozone destruction, but it also reduces the rate of $ClONO_2$ recovery after PSCs processing, conserving high Cl_x, which destroys ozone.
Three-dimensional Eulerian off-line models, forced by meteorological analyses, are widely used to simulate these processes and to present time and space distribution of chemical species [Chipperfield et. al., 1993; Lefevre et al., 1994]. However, Lagrangian view on atmospheric motion is also used for visualization of tracer field [Sutton, 1994] and trajectory mapping of the satellite data [Morris et. al., 1995].

Lutman et. al., [1997] integrated chemistry along a large number of domain-filling forward trajectories, but air parcels in this case tend to disperse irregularly. The reverse domain-filling trajectories with chemistry allow to get the values of species on regular grid [Schoerberl et. al., 1996].
This approach has been used in our model.

2. Model description

The continuity equation with no diffusion for a species *i*, with concentration n_i, is written:

$$\frac{\partial n_i}{\partial t} + \nabla(n_i \bar{v}) = P_i - L_i n_i \qquad (1)$$

where:
$\bar{v}$ - velocity vector;
P_i and L_i - source and sink of *i* -th specie respectively.

In terms of mixing ratio $\mu_i = \frac{n_i}{N}$, where N is air concentration, (1) will be written:

$$\frac{d\mu_i}{dt} = \frac{P_i}{N} - L_i \mu_i \qquad (2)$$

where:
$\frac{d\mu_i}{dt} = \frac{\partial \mu_i}{\partial t} + \bar{v}\nabla\mu_i$ - full Lagrangian derivative.
Therefore an integration of (2) can be conducted in two stages:
- An air parcel trajectory calculation;
- The chemical box model integration along this trajectory.

No interaction between air parcels is suggested, i.e. the atmospheric motion is considered as the large amount of tubes (parcel trajectories) with nontransparent walls.

2.1. Trajectory calculation.

The time integration of particle advection equation expressed in spherical coordinates is performed using a fourth-order Runge-Kutta method with linear interpolated in time and space ECMWF analyzed winds. Isentropic trajectories are calculated keeping fixed potential temperature, while for full three-dimensional trajectories the vertical winds from ECMWF analyses are used. In this study data with 2.5x2.5 degree space and 12 hours time resolutions are used for 3-d trajectory calculation. To avoid inaccuracies near the poles, for latitudes exceeded 70 N and –70 S, the integration is conducted using Cartesian coordinates.

2.2. Chemical box model.

The chemical box model includes 36 species:
O_3, O, O (^{1}D), H, OH, HO_2, H_2O, H_2O_2, NO, NO_2, NO_3, N_2O_5, HNO_3, HNO_4, Cl, Cl_2, ClO, Cl_2O_2, OClO, HCl, $ClONO_2$, HOCl, $ClNO_2$, CO, CH_4, CHO, CH_2O, CH_3O, CH_3O_2, CH_3O_2H, Br, BrO, BrCl, $BrONO_2$, HBr, HOBr
Families:

$O_x = O_3 + O(^1D) + O(^3P)$;

$NO_x = NO + NO_2 + NO_3$;

$Cl_x = Cl + ClO + 2Cl_2O_2$;

$Br_x = Br + BrO$

84 homogeneous chemical reactions and 32 photolysis reactions are considered, rate constants and absorption cross sections are taken from DeMore *et al.*, [1997].

The values of N_2, O_2, H_2 are fixed in the model.

Long-lived species and families are integrated in time by backward differentiation formula:

$$\mu_i^{n+1} = \frac{\mu_i^n + \Delta t \overline{P_i^{n+1}}}{1 + \Delta t L_i^{n+1}} \qquad (3)$$

where:

$\Delta t = t^{n+1} - t^n$;

$\overline{P} = \frac{P}{N}$

This implicit scheme is resolved by Gauss-Seidel iteration as in Verwer *et al.*, [1996], while for short-lived species equilibrium conditions are applied on every time step and also resolved iteratively. The application of Gauss-Seidel technique permits to solve the implicit scheme explicitly (no need to solve systems of equations like in case of Newton iteration, for example). The number of Gauss-Seidel iterations depends on the needed accuracy. Reduction of Δt below 10 min. doesn't affect output results for 10-day integration, thus a time step of 10 minutes is used in the model.

PSCs type I and II are allowed to form when the temperature becomes lower than the threshold temperature for nitric acid trihydrate (NAT) particles [Hanson and Mauersberger , 1988] or water ice (ICE) particles [Murray, 1967]. Fixed radius for PSCs are assumed (1 μm for type I, 10 μm for type II) for calculation of available surface area. Supercooled liquid particles are not included into the model yet.

Model contains 5 heterogeneous reactions on PSCs:

$N_2O_5 + H_2O \rightarrow 2HNO_3$; (H1)

$N_2O_5 + HCL \rightarrow CLNO_2 + HNO_3$; (H2)

$CLONO_2 + H_2O \rightarrow HOCL + HNO_3$; (H3)

$CLONO_2 + HCL \rightarrow CL_2 + HNO_3$; (H4)

$HOCL + HCL \rightarrow CL_2 + H_2O$ (H5)

(H1) and (H3) take place on the background sulfate aerosol also.

The uptake coefficients are taken from [DeMore *et al.*, 1997].

3. Results and discussion

On March, 10, 1997 a total of 1632 three-dimensional 11-days backward trajectories have been initialized on the regular grid between 50 N and 90 N latitude circles and potential temperature level at 480 K . Then chemical species initialized on the same level at the end points of these backward trajectories on February, 28, 1997 have been advected forward in time to initial grid points with updating their values from box model calculation every time step.

Initial chemical species mixing ratios for this study have been taken from 3-D SLIMCAT model (Cambridge Univ.). Results are presented in Figure 1. The region of gas phase nitric acid conversion to solid form consists with the low temperature region. The shape of $ClONO_2$ consumption, chlorine activation and ozone depletion areas is the same. Therefore the species distribution pattern is realistic enough. To get the vertical structure this procedure should be repeated for different potential temperature levels.

This Lagrangian approach has some advantages:

- no numerical diffusion, which produces spurious mixing of species;
- to get higher field resolution only larger amount of trajectories is needed;
- it is possible to investigate the evolution of any specie along the trajectory.

The main disadvantage is inaccuracy for long-duration trajectories, due to time and space resolution, interpolation and accuracy of the analyzed data, especially vertical winds. For this reason such simulation for periods longer than a month is not very reliable.

Therefore Lagrangian model should be considered as complementary to Eulerian one.

As it has been noted, the Lagrangian approach allows to investigate the evolution of the temperature, solar irradiation and mixing ratio of the species along the trajectory. We conducted the model studies of ozone loss rate sensitivity to sunlight and PSCs coexistence.

This study focuses on the single short sunlight and PSCs interaction, which determines ozone loss rate. For different initial mixing ratios of NO_x and N_2O_5 two model runs have been conducted. Run A corresponds to joint sunlight and PSCs processing, while in run B the same trajectory is analyzed, but sunlight appears later than PSCs.

The typical isentropic 10-day trajectory of 435 K level has been chosen, because, as it is shown on Figure 2, there is a short period of PSCs and sunlight coexistence on this trajectory. To study the effect of such interaction on species behavior the integration also has been performed without this sunlit period (run B, right panel of Figure 2). Left panel of the figure shows the real trajectory (run A).

Initial mixing ratios of the species are taken as not disturbed by PCSs yet, i.e. high $ClONO_2$ (0.6 ppbv), HCl (2.1 ppbv) and low Cl_x (0.2 ppbv), high NO_x (1 ppbv) and N_2O_5 (1 ppbv).

In run A during the period of PSCs processing with no sunlight HCL and $ClONO_2$ are partly consumed due to heterogeneous reactions, then in presence of sunlight $ClONO_2$ recovery through reaction:

$$ClO + NO_2 + M \rightarrow ClONO_2 + M$$

becomes stronger, because photolysis of N_2O_5, $ClNO_2$ and Cl_2 provides additional NO_x and Cl_x. During the last stage of PSCs processing without sunlight HCl and $ClONO_2$ are consumed again. The active chlorine increases during sunlight and PSCs coexistence via photolysis of temporal reservoirs Cl_2 and $ClNO_2$, leading to ozone depletion.

Meanwhile in run B the ozone loss rate decreases significantly, because of fast $ClONO_2$ recovery during next sunlit period, preventing chlorine activation.

Figure 3 shows the same experiment results, but for the denoxified air parcel (initial NO_x and N_2O_5 equal 0.05 ppbv). Chlorine activation in this case is stronger than $ClONO_2$ recovery in run B during first sunlit period after PSCs and the further ozone behavior is almost the same as in run A, although the absolute ozone loss rate is higher in both cases than in Figure 2.

Since an atmosphere is not denoxified, as inside early vortex or outside one, ozone loss rate increases significant in case of sunlight and PSCs coexistence. This effect is negligible for denoxified air parcel, typical for late winter inside vortex.

The another model sensitivity study regards the temperature dependence of ozone loss rate. Substantial biases (~ 5 degrees) between ECMWF and UKMO analyzed and observed temperatures in the arctic winter lower stratosphere have been found [Knudsen, 1996]. Usually this is coursed by adiabatic displacements of air parcels due to wave activity over mountain areas.
We compared the results of model integration along two trajectories, where temperatures differ on 5 degrees. Results are presented in Figure 4. The temperature decrease leads to significant increase of ozone loss rate (from 18 ppbv/day to 28 ppbv/day) because of increase of PSC I surface area and existing PSC II.

4. Summary

A Lagrangian multi-trajectory chemical model reproduces the general behavior of ozone-active species in Arctic region in winter-spring season, such as chlorine activation on PSCs, ozone depletion and chlorine reservoirs recovery.
Reverse domain-filling (RDF) technique with chemistry makes it possible to get the species mixing ratio values on the regular grid and provides the high field resolution with no artificial mixing between air parcels. To increase this resolution only larger amount of trajectories is needed. Therefore this method can be used to obtain the fine structure of tracer distribution in the region of interest. The advantage of RDF over Eulerian (grid) models is that there is no numerical diffusion and, as a result, no spurious smoothing of the tracer field.
Ozone loss rate sharply increases inside the air parcel processed by PSCs and sunlight simultaneously, if this air parcel is not denoxified.
Temperature decrease in 5 degree along one 11-day selected trajectory leads to ozone loss rate increase from 18 ppbv/day to 28 ppbv/day.

References

Chipperfield , M.P., D. Cariolle, P. Simon, R. Ramaroson, D.J. Lary, A three-dimensional modeling study of trace species in the Arctic lower stratosphere during winter 1989-1990, *J. Geophys. Res.*, 98, 7199-7218, 1993.

DeMore W.B., S.P. Sander, D.M. Golden, R.F. Hampson, M.J. Kurylo, C.J. Howard, A.R. Ravishankara, C.E. Kolb, M.J. Molina, Chemical Kinetics and Photochemical Data for use in Stratospheric Modeling, Evaluation 12, *NASA JPL Publ.* 97-4, 1997.

Hanson, D.R., K. Mauersberger, Vapour-pressures of HNO_3 / H_2O solutions at low temperatures, *J. Phys. Chem.*, 92, 6167-6170, 1988.

Knudsen, B. M., Accuracy of arctic stratospheric temperature analyses and the implications for the prediction of polar stratospheric clouds, *Geophys. Res. Lett.*, 25, 3747-3750, 1996.

Lefevre, F., G. P. Brasseur, I. Folkins, A. K. Smiith, and P. Simon, Chemistry of the 1991-1992 stratospheric winter: Three-dimensional model simulations, *J. Geophys. Res.*, 99, 8183-8195, 1994.

Luthman, E.R., J.A. Pyle, M.P. Chipperfield, D.J. Lary, I. Kilbane-Dawe, J.W. Waters, N. Larsen, Three-dimensional studies of the 1991/1992 northern hemisphere winter using domain-filling trajectories with chemistry, *J. Geophys. Res.*, 102, D1, 1479-1488, 1997.

Morris, G. A., M. R. Schoeberl, L. C. Sparling, P. A. Newman, L. R. Lait, L. Elson, J. Waters, R. A. Suttie, A. Roche, J. Kumer, and J. Russel, III, Trajectory mapping and applications to data from the Upper Atmospheric Research Satellite, *J. Geophys. Res.*, 100, 16,491-16,505,

1995.
Murray, F.W., On the computation of saturation vapour pressure, *J. Appl. Met.*, 6, 203-204, 1967.
Shoeberl, M.R., A.R. Douglass, S.R. Kawa, A.E. Dessler, P.A. Newman, R.S. Stolarski, A.E. Roche, J.W. Waters, J.M. Russell, Development of the Antarctic ozone hole, *J. Geophys. Res.*, 101, 20,909-20,924, 1996.
Verwer, J.G., J.G. Blom, M. Van Loon, E.J. Spee, A comparison of stiff ODE solvers for atmospheric chemistry problems, *Atmos. Environment*,vol. 30, No 1, pp. 49-58,1996.

Figure Captions:

Figure 1. Reverse domain-filling trajectories (number of trajectories: 1632, duration: 11 days, potential temperature level: 480 K, latitude range: 50N-90N).

Figure 2. Ozone loss rate sensitivity to sunlight and PSCs coexistence (NO_x (1 ppbv), N_2O_5(1 ppbv)).

Figure 3. The same as Figure 1, but (NO_x (0.05 ppbv), N_2O_5(0.05 ppbv)).

Figure 4. Temperature dependence of ozone loss rate.

T (K)

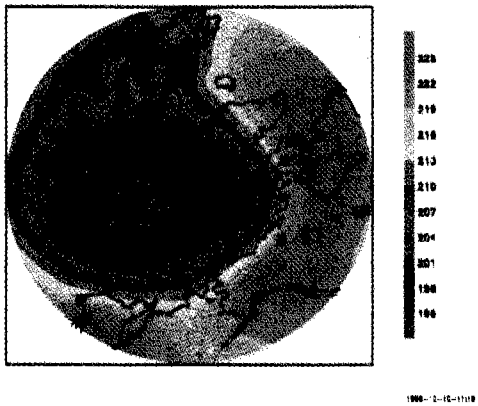

HNO3 (g) (ppbv)

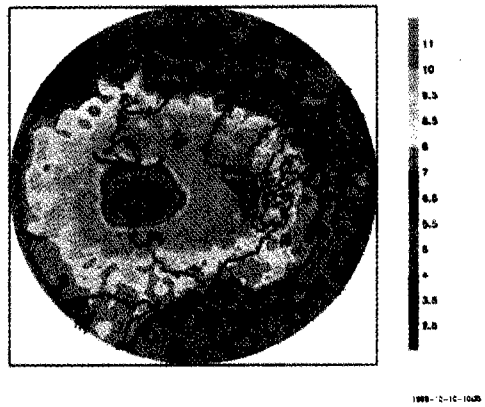

HCl (ppbv)

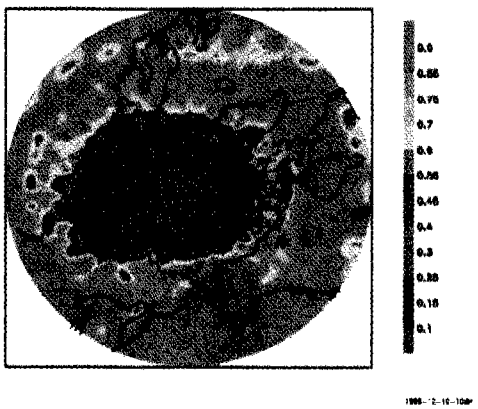

ClONO2 (ppbv)

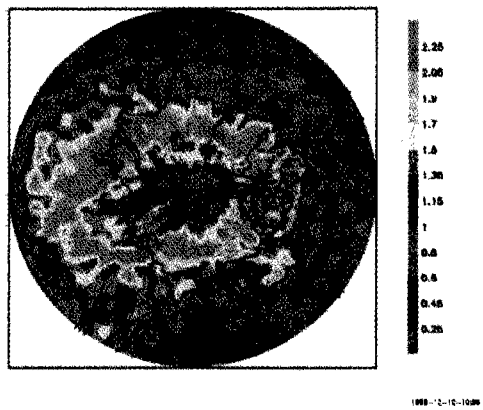

Clx (ppbv)

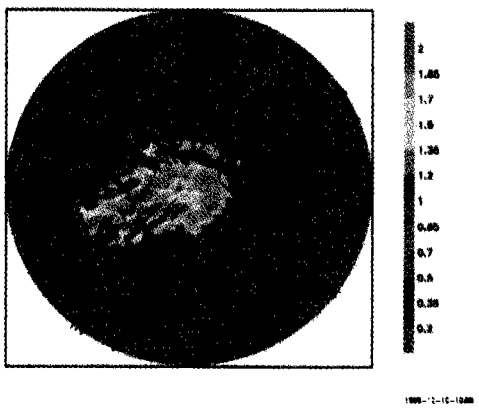

O3 (ppmv)

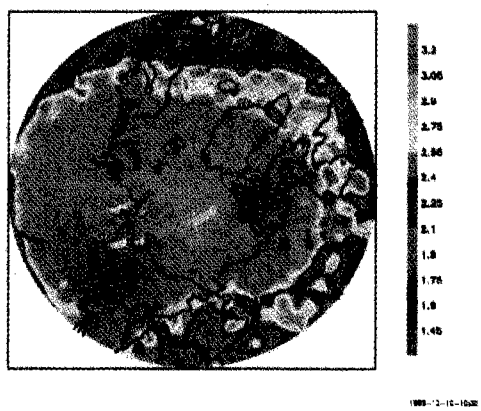

Figure 1

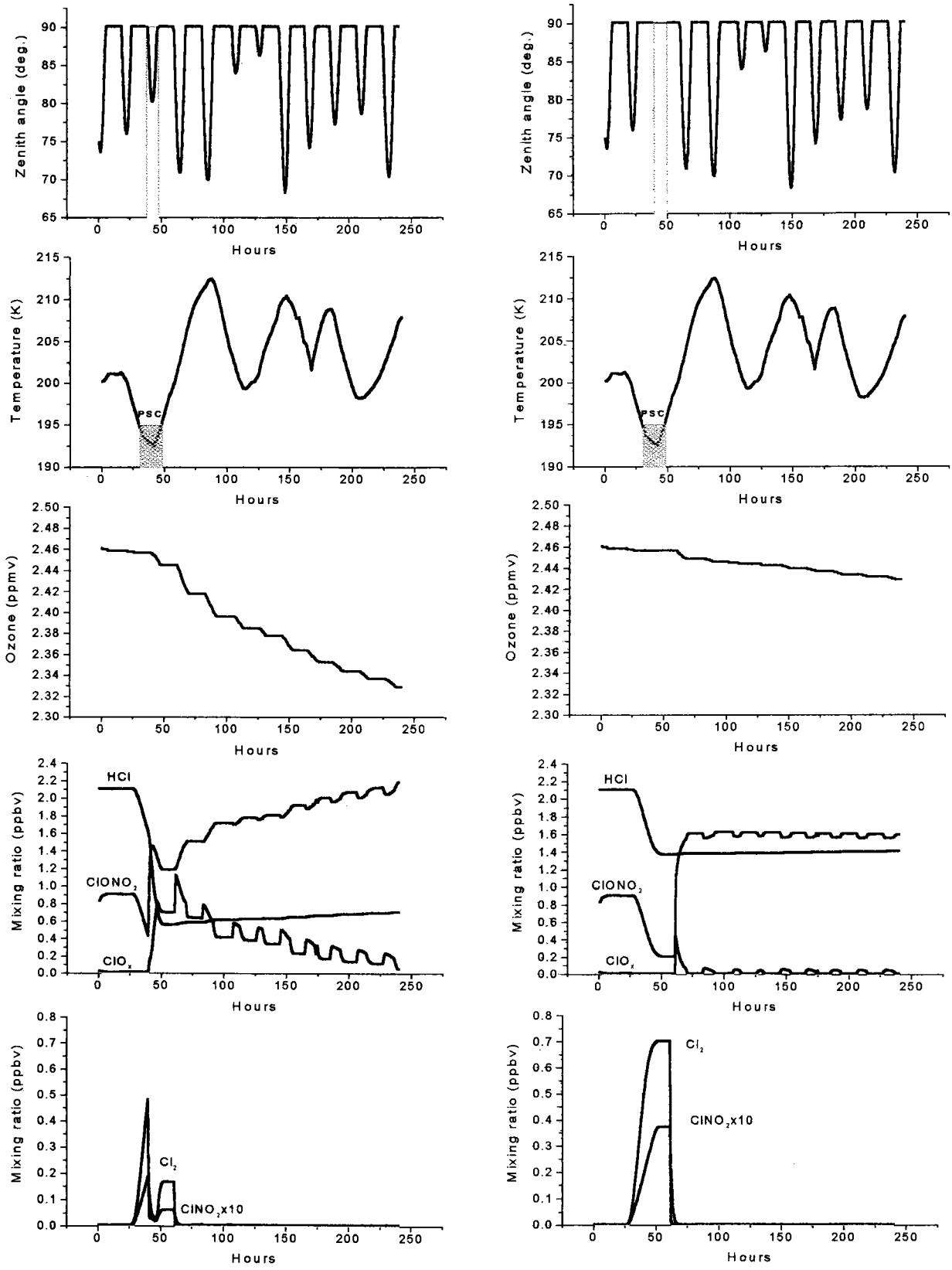
Zenith angle (deg.)
Hours
Temperature (K)
PSC
Ozone (ppmv)
Mixing ratio (ppbv)
HCl
ClONO2
ClOx
Cl2
ClNO2x10

Figure 2

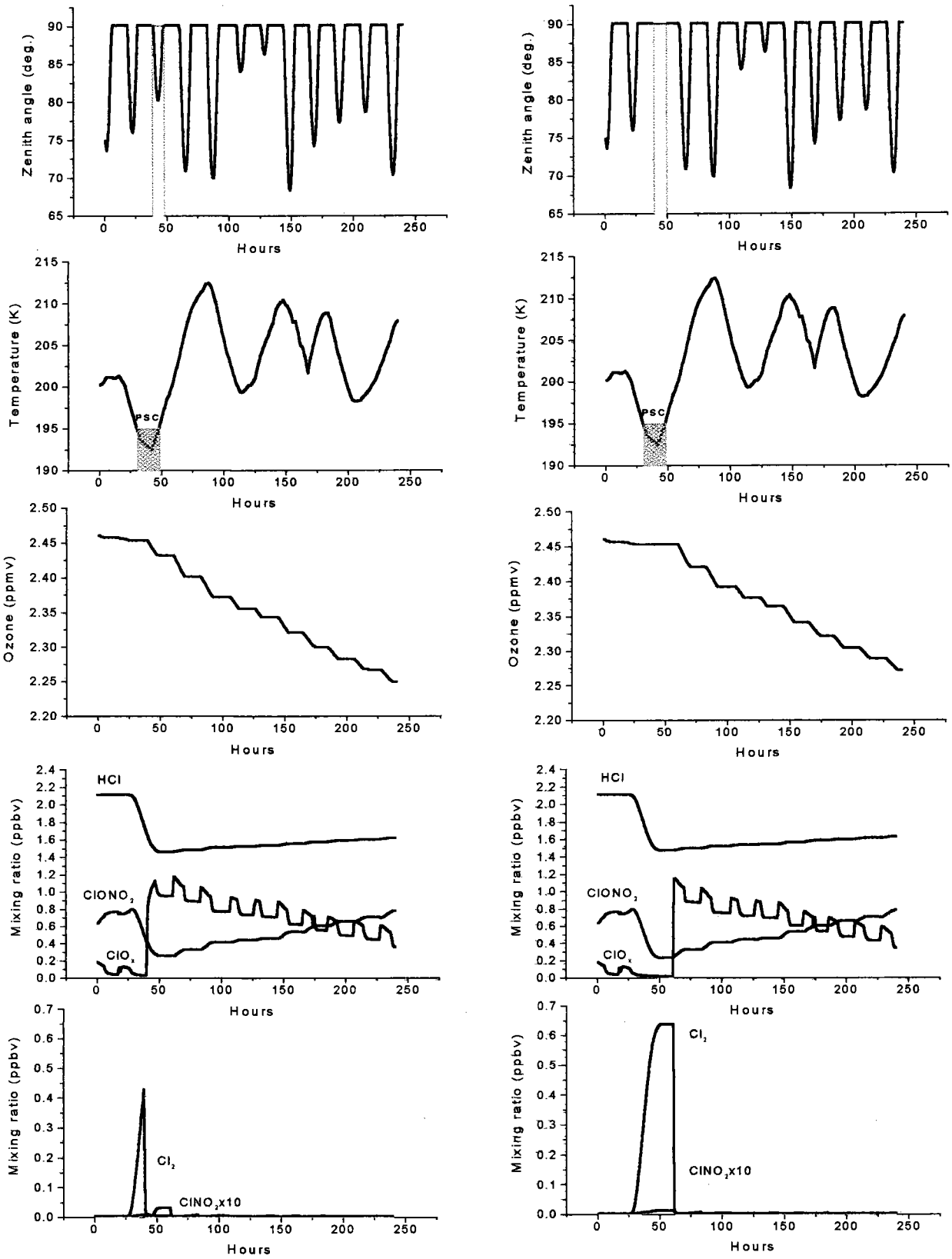
Zenith angle (deg.)
Hours
Temperature (K)
PSC
Ozone (ppmv)
Mixing ratio (ppbv)
HCl
ClONO2
ClOx
Cl2
ClNO2x10

Figure 3

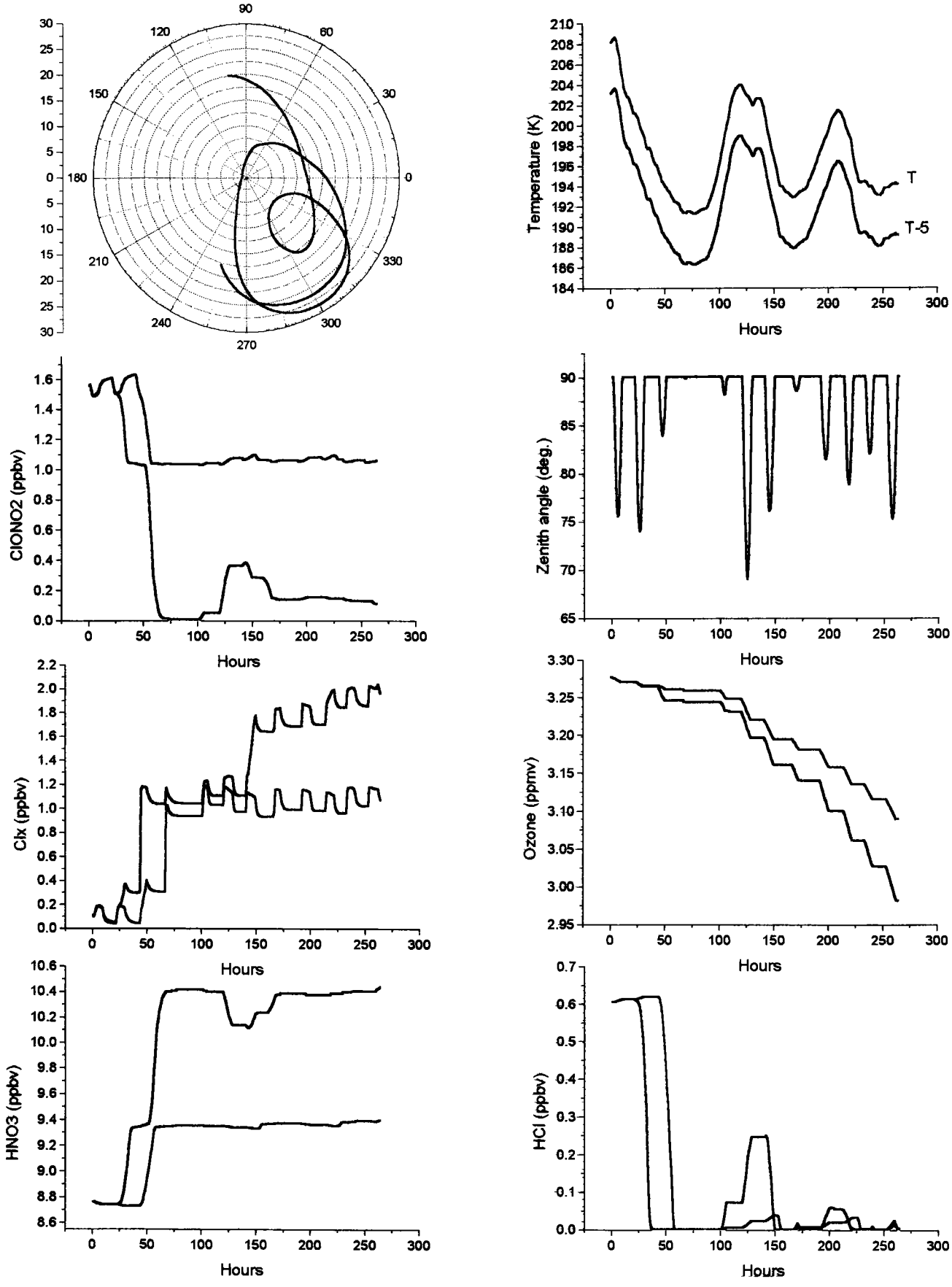
90
120
60
150
30
180
0
210
330
240
300
270
Temperature (K)
T
T-5
Hours
ClONO2 (ppbv)
Hours
Zenith angle (deg.)
Hours
Clx (ppbv)
Hours
Ozone (ppmv)
Hours
HNO3 (ppbv)
Hours
HCl (ppbv)
Hours

Figure 4